

**Supplementary Table 1.** Genomic analysis of ovarian cancer patient samples (n=87) and cell lines (n=34) shows that *PIK3CA* mutant samples commonly exhibit secondary mutations in *PTEN*, *KRAS* or *PIK3R1*.

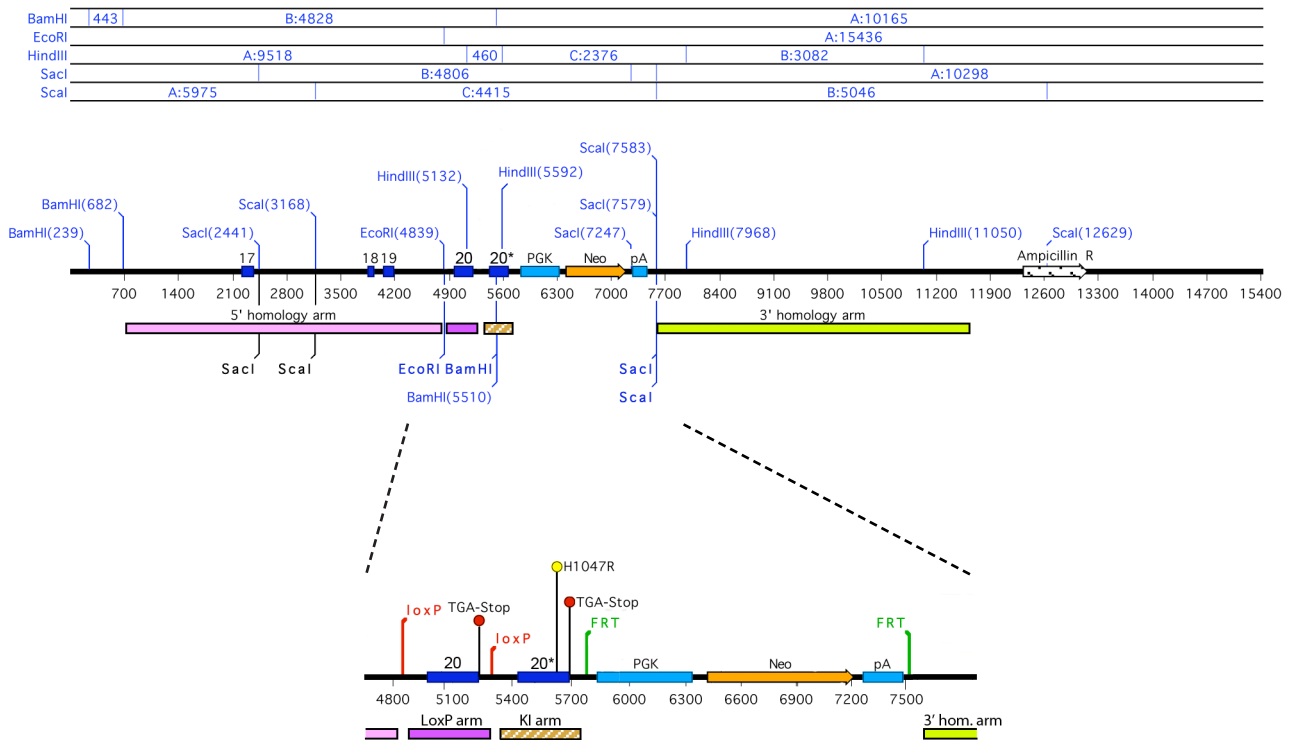
	<i>PIK3CA</i>	<i>PIK3R1</i>	<i>PTEN</i>	<i>KRAS</i>
<u>Primary patient samples</u>				
32068	H1047R		R130G	
60093	E542K		Y138D(+)P190L (+)K267fsX275	
23043	H1047R			G12V
IC359	E726K	E403_L405 delinsD	R130G	
IC580	H1047R			
IC349	H1047R			
IC131	H1047R			
P1921	E542K			
P0706	E542K			
IC128	K111E			
IC526		N564fsX712	R130X(+)L146X	
P1768		c.1425+1G>T	G132V	
P4881		c.1426-2delAG		
P5390			HD	G12V
22061			R233X	G12V
IC594			HD	
P4219			HD	
IC095	AMP			
IC293	AMP			
IC399	AMP			
IC434	AMP			
P0505	AMP			
IC086	AMP			
IC315	AMP			
IC489	AMP			
IC551	AMP			
P1094				G12V
P1977				G12C
IC080				G12V
IC138				G13D
IC257				G13D
IC343				G12D
<u>Cell lines</u>				
IGROv1	Stop1069W	n.d	955-958del	
TOV-21G	H1047Y	n.d	Protein loss <sup>A</sup>	G13C <sup>B</sup>
MCAS	H1047R	n.d		G12D
OAW42	H1047L	n.d		
SKOV-3	H1047R	n.d		
JHOC-7	E542K	n.d		
2008	E545K	n.d		
A2780		n.d	K128_R130del	
EFO-27		n.d	800delA (fs)	
JHOM-1		n.d	Protein loss <sup>A</sup>	
Colo704		n.d	Protein loss <sup>A</sup>	
Colo720E		n.d	Protein loss <sup>A</sup>	
CAOV3	AMP	n.d		
OWA28	AMP	n.d		
EFO21	AMP	n.d		
SW626		n.d		G12V <sup>B</sup>
OVCAR-5		n.d		G12V <sup>B</sup>

<sup>A</sup>, western blot; <sup>B</sup>, Sanger database; n.d. not determined; HD, homozygous deletion; AMP, amplification, log<sub>2</sub> ratio threshold of >0.6 (high level gain)

**Supplementary Table 2.** Observed versus expected genotypes from crosses of mice heterozygous for the *Pik3ca*<sup>Lat-H1047R</sup> allele

Genotype		<i>Pik3ca</i> <sup>Lat-H1047R/wt</sup> x <i>Pik3ca</i> <sup>Lat-H1047R/wt</sup>	
		Observed <sup>a</sup>	Expected
<i>Pik3ca</i> <sup>wt/wt</sup>	Male	13 (11.3%)	12.5%
	Female	10 (8.7%)	12.5%
	<b>TOTAL</b>	<b>23 (20.0%)</b>	<b>25.0%</b>
<i>Pik3ca</i> <sup>Lat-H1047R/wt</sup>	Male	26 (22.6%)	25.0%
	Female	35 (30.4)	25.0%
	<b>TOTAL</b>	<b>61 (53.0%)</b>	<b>50.0%</b>
Homozygous <i>Pik3ca</i> <sup>Lat-H1047R</sup>	Male	18 (15.7%)	12.5%
	Female	13 (11.3%)	12.5%
	<b>TOTAL</b>	<b>31 (27.0%)</b>	<b>25.0%</b>

<sup>a</sup> n=115 pups from 24 litters. Numbers observed with percentage in parentheses.



**Supplementary figure 1: *Pik3ca*<sup>Lat-H1047R</sup> targeting construct.** A schematic of the genomic structure of the *Pik3ca*<sup>Lat-H1047R</sup> allele showing the 4 fragments used to generate the targeting construct; the 5' homology arm (pink), the loxP arm (purple) incorporating the wild type exon 20 flanked by loxP sites and containing an EcoR1 site at the 5' end for genomic screening, the knock-in (KI, orange) arm incorporating a duplicate copy of exon 20 incorporating the H1047R (CAT→AGG) mutation, a number of silent sequence changes to facilitate genotyping and a BamH1 site for genomic screening, and the 3' homology arm (light green). Also shown are the relative locations of *Pik3ca* exons 17-20 (dark blue boxes) and the inserted mutant exon 20 (20\*), the loxP (red) and FRT (green) sites, stop codons (red circles) and H1047R mutation (yellow circle), the PGK-neomycin selection cassette (cyan and orange boxes) and various restriction enzyme sites (light blue). The grid at the top indicates the size (bp) of the fragments obtained following digestion of the *Pik3ca*<sup>Lat-H1047R</sup> allele with each of the restriction enzymes.

<b>Wild type exon 20</b>	G	TTT	CAG	GAG	ATG	TGT	TAC	AAG	GCT	TAC
	<b>F</b>	<b>Q</b>	<b>E</b>	<b>M</b>	<b>C</b>	<b>Y</b>	<b>K</b>	<b>A</b>	<b>Y</b>	
<b>Mutant exon 20</b>	G	TTT	CAG	GAG	ATG	TGT	TAC	AAG	GCT	TAC
	<b>F</b>	<b>Q</b>	<b>E</b>	<b>M</b>	<b>C</b>	<b>Y</b>	<b>K</b>	<b>A</b>	<b>Y</b>	

---

CTA	GCA	ATT	CGG	CAG	CAT	GCC	AAT	CTC	TTC	ATC	AAC	CTT	TTT
<b>L</b>	<b>A</b>	<b>I</b>	<b>R</b>	<b>Q</b>	<b>H</b>	<b>A</b>	<b>N</b>	<b>L</b>	<b>F</b>	<b>I</b>	<b>N</b>	<b>L</b>	<b>F</b>
CTA	GCA	ATT	CGG	CAG	CAT	GCC	AAT	CTC	TTC	ATC	AAC	CTT	TTT
<b>L</b>	<b>A</b>	<b>I</b>	<b>R</b>	<b>Q</b>	<b>H</b>	<b>A</b>	<b>N</b>	<b>L</b>	<b>F</b>	<b>I</b>	<b>N</b>	<b>L</b>	<b>F</b>

---

TCA	ATG	ATG	CTT	GGC	TCT	GGA	ATG	CCA	GAA	CTA	CAA	TCT	TTT
<b>S</b>	<b>M</b>	<b>M</b>	<b>L</b>	<b>G</b>	<b>S</b>	<b>G</b>	<b>M</b>	<b>P</b>	<b>E</b>	<b>L</b>	<b>Q</b>	<b>S</b>	<b>F</b>
TCA	ATG	ATG	CTT	GGC	TCT	GGA	ATG	CCA	GAA	CTA	CAA	TCT	TTT
<b>S</b>	<b>M</b>	<b>M</b>	<b>L</b>	<b>G</b>	<b>S</b>	<b>G</b>	<b>M</b>	<b>P</b>	<b>E</b>	<b>L</b>	<b>Q</b>	<b>S</b>	<b>F</b>

---

GAT	GAC	ATT	GCA	TAT	ATC	CGA	AAG	ACT	CTA	GCC	TTG	GAC	AAA
<b>D</b>	<b>D</b>	<b>I</b>	<b>A</b>	<b>Y</b>	<b>I</b>	<b>R</b>	<b>K</b>	<b>T</b>	<b>L</b>	<b>A</b>	<b>L</b>	<b>D</b>	<b>K</b>
GAT	GAC	ATT	GCA	TAT	ATC	CGA	AAG	ACT	CTA	GCC	TTG	GAC	AAA
<b>D</b>	<b>D</b>	<b>I</b>	<b>A</b>	<b>Y</b>	<b>I</b>	<b>R</b>	<b>K</b>	<b>T</b>	<b>L</b>	<b>A</b>	<b>L</b>	<b>D</b>	<b>K</b>

---

ACT	GAG	CAA	GAA	GCT	TTG	GAA	TAT	TTC	ACA	AAG	CAA	ATG	AAT
<b>T</b>	<b>E</b>	<b>Q</b>	<b>E</b>	<b>A</b>	<b>L</b>	<b>E</b>	<b>Y</b>	<b>F</b>	<b>T</b>	<b>K</b>	<b>Q</b>	<b>M</b>	<b>N</b>
ACT	GAG	CAA	GAA	GCT	TTG	GAA	TAT	TTC	ACA	AAG	CAA	ATG	AAT
<b>T</b>	<b>E</b>	<b>Q</b>	<b>E</b>	<b>A</b>	<b>L</b>	<b>E</b>	<b>Y</b>	<b>F</b>	<b>T</b>	<b>K</b>	<b>Q</b>	<b>M</b>	<b>N</b>

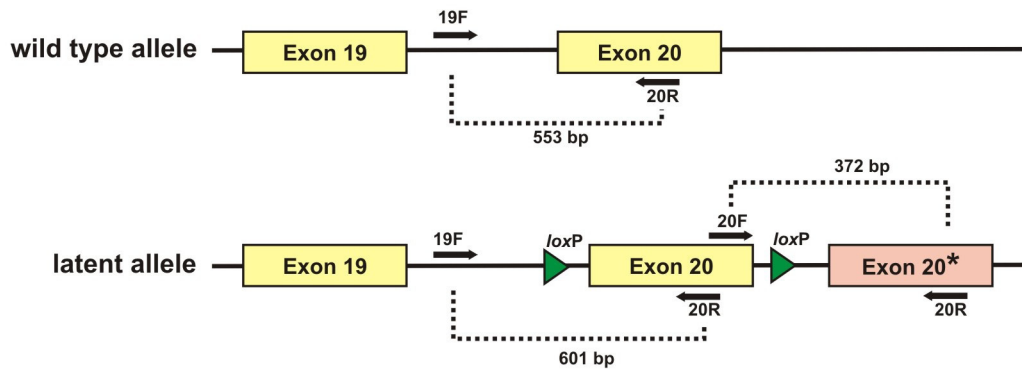
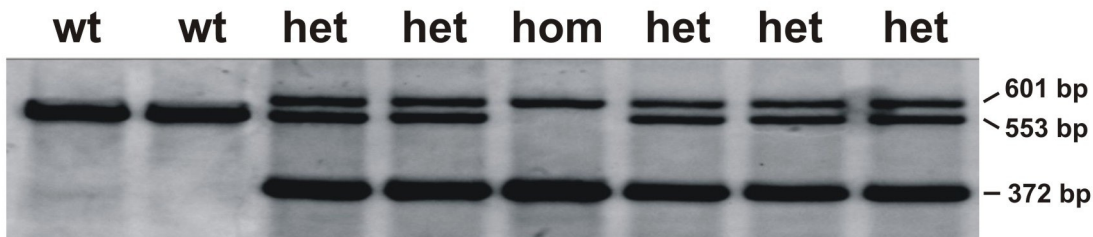
---

GAT	GCA	CAT	CAT	GGT	GGA	TGG	ACG	ACA	AAA	ATG	GAT	TGG	ATC
<b>D</b>	<b>A</b>	<b>H</b>	<b>H</b>	<b>G</b>	<b>G</b>	<b>W</b>	<b>T</b>	<b>T</b>	<b>K</b>	<b>M</b>	<b>D</b>	<b>W</b>	<b>I</b>
GAC	GCT	AGG	CAC	GGA	GGG	TGG	ACG	ACA	AAA	ATG	GAT	TGG	ATC
<b>D</b>	<b>A</b>	<b>R</b>	<b>H</b>	<b>G</b>	<b>G</b>	<b>W</b>	<b>T</b>	<b>T</b>	<b>K</b>	<b>M</b>	<b>D</b>	<b>W</b>	<b>I</b>

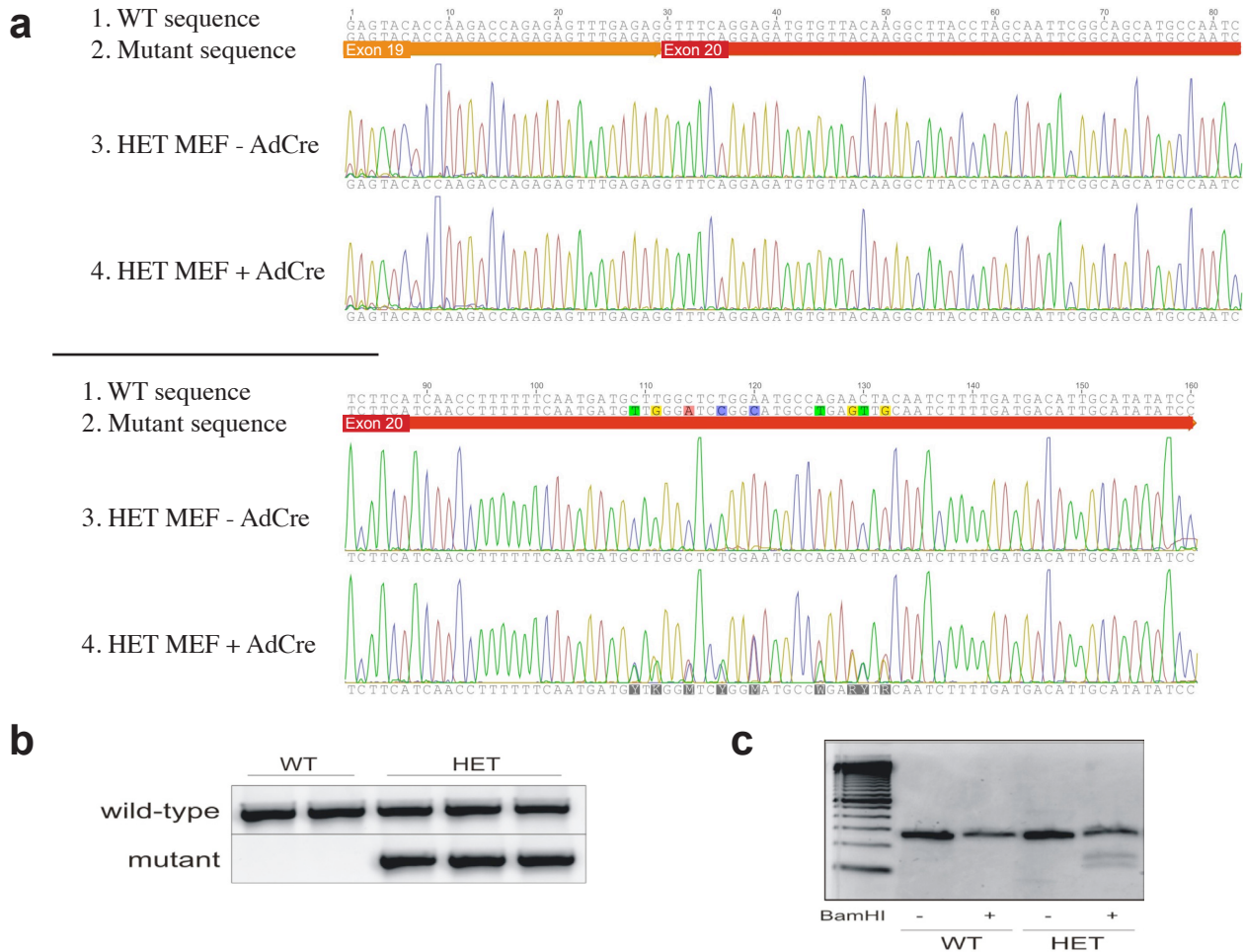
---

TTC	CAC	ACC	ATC	AAG	CAG	CAT	GCT	TTG	AAC	TGA
<b>F</b>	<b>H</b>	<b>T</b>	<b>I</b>	<b>K</b>	<b>Q</b>	<b>H</b>	<b>A</b>	<b>L</b>	<b>N</b>	<b>stop</b>
TTC	CAC	ACC	ATC	AAG	CAG	CAT	GCT	TTG	AAC	TGA
<b>F</b>	<b>H</b>	<b>T</b>	<b>I</b>	<b>K</b>	<b>Q</b>	<b>H</b>	<b>A</b>	<b>L</b>	<b>N</b>	<b>stop</b>

**Supplementary figure 2: DNA and protein sequences of the wild type and mutant versions of exon 20.** The red box identifies the CAT→AGG (H→R) mutation (blue), the black boxes indicate regions incorporating silent base changes (pink) and the orange shading indicates the BamH1 restriction enzyme site in the mutant exon.

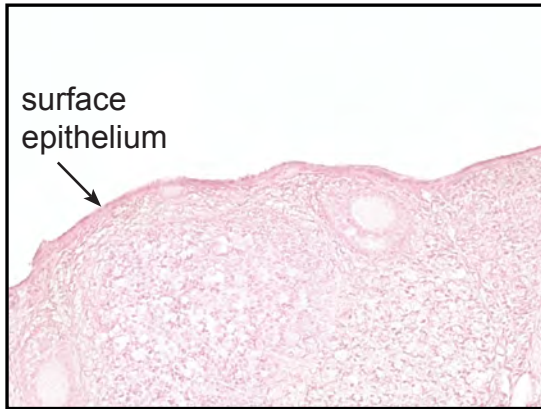
**a****b**

**Supplementary Figure 3: Genotyping using a PCR-based strategy. (a)** Schematic diagram of the genomic structure of the WT and latent *Pik3ca*<sup>H1047R</sup> alleles showing the WT exons 19 and 20 (yellow boxes), the *loxP* sites (green triangles) and the mutant version of exon 20 (exon 20\*, pink). Primer binding sites are indicating arrows. **(b)** Genomic DNA (0.5 $\mu$ l) extracted from mice was mixed with 30ng of each of primers 19F, 20F and 20R, 2.5mM dNTPs and 0.05 $\mu$ l Gotaq polymerase (Promega) in a total of 10 $\mu$ l Gotaq buffer and amplified at 95 $^{\circ}$ C for 10min followed by 95 $^{\circ}$ C for 30sec, 55 $^{\circ}$ C for 30sec, 72 $^{\circ}$ C for 40sec for 35 cycles and then 72 $^{\circ}$ C for 5min. The amplified product was then run on 2% agarose gel (150V, 70min) and stained with ethidium bromide. Shown are the results from 8 representative mice. Primer sequences: 19F (5'-TTGGTTC-CAGCCTGAATAAAGC-3'), 20F (5'-TCCACACCATCAAGCAGCA-3') and 20R (5'-GTCCAAGGC-TAGAGTCTTTCGG-3').

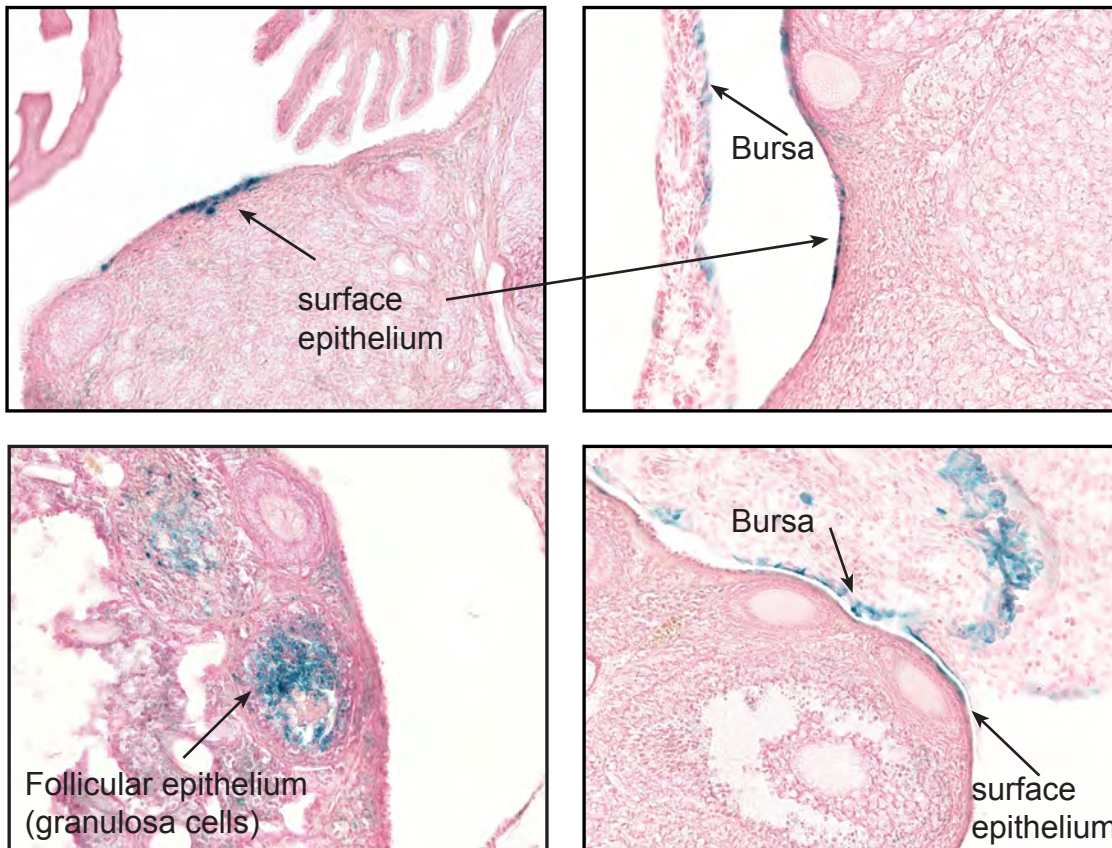


**Supplementary figure 4: Knock-in of mutant exon 20 in MEFs.** Cre-mediated knock-in of the mutant exon 20 was confirmed by sequencing, allele-specific PCR and restriction digestion using MEFs from mice heterozygous for the latent *Pik3ca*<sup>H1047R</sup> allele (HET) and infected with AdCre. RNA from control (-AdCre) and AdCre infected (+AdCre) WT and HET MEFs was reverse transcribed into cDNA. **(a) Sequencing:** cDNA was sequenced from exon 19 into exon 20 (ex19-specific primer: 5'-CAAGAGTACACCAAGACCAGAGAGTT-3') and confirmed by sequencing from exon 20 (5'-TCCAATCCATTTTTGTCGTCC-3'). Shown are the expected sequences and sequencing traces for cDNA from HET MEFs with or without AdCre. The cDNA sequence from the AdCre-treated MEFs is heterozygous at the sites of silent base changes engineered into the mutant exon 20. **(b) Allele-specific PCR:** cDNA from AdCre-treated wild type or HET MEFs was amplified by using primers (19F: 5'-CAAGAGTACACCAAGACCAGAGAGTT-3') and (WT20R: 5'-TGTCGTCCATCCACCATGATGT-3') or (Mut20R 5'-TGTCGTCCACCCTCCGTGCCTA-3'). **(c) Restriction digestion:** cDNA from AdCre-treated WT or HET MEFs was amplified using primers (19F: 5'-CAAGAGTACACCAAGACCAGAGAGTT-3') and (Com20R: 5'-TCCAATCCATTTTTGTCGTCC-3') and the 268 bp product digested with BamH1. The product derived from the wild type cDNA is not cut by BamH1 but the product from cDNA incorporating the mutant exon 20 is cut into two fragments of 153 bp and 115 bp.

## Right ovary (No AdCre)

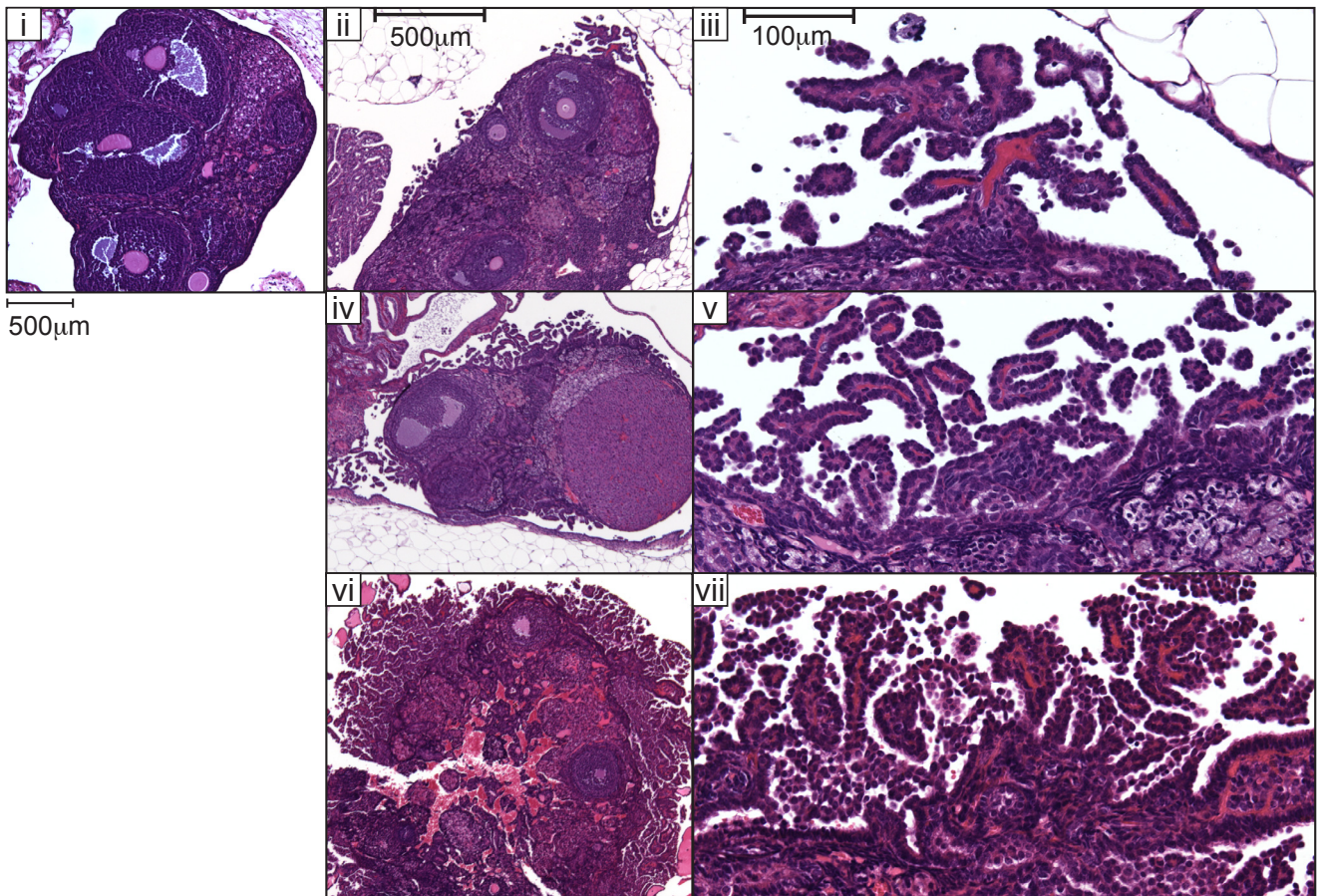


## Left ovary (+ intrabursal AdCre)



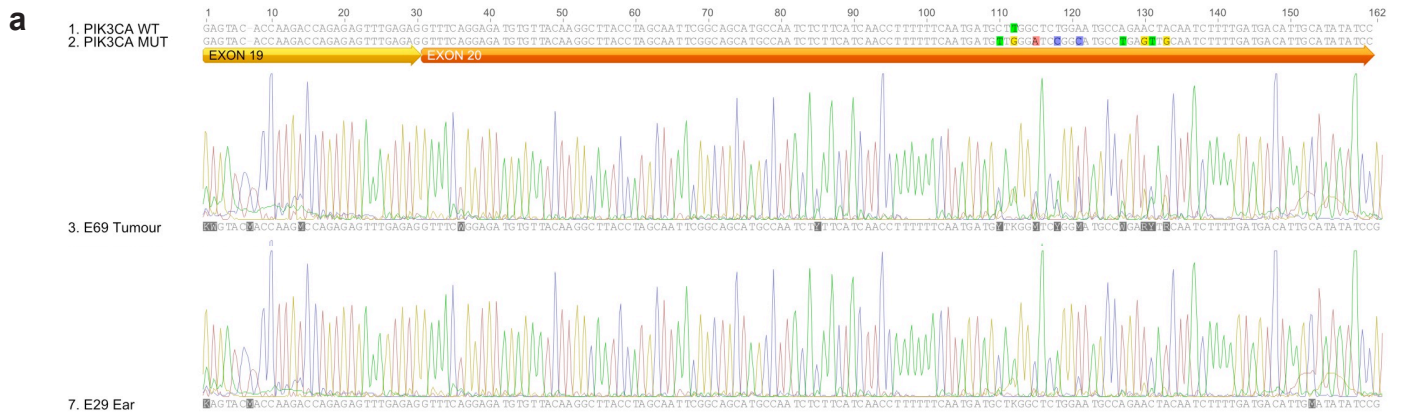
**Supplementary figure 5.  $\beta$ -galactosidase staining following intrabursal AdCre injection in LSL-LacZ mice.**

LSL-LacZ (Rosa) reporter mice were superovulated and 5 $\mu$ L of Ad-Cre was injected into the left intra-ovarian-bursa cavity. Following 72 Hours infection, the mice were sacrificed and each ovary and adjacent tissues were isolated. Tissues were fixed and stained for  $\beta$ -galactosidase activity. AdCre infected cells with successful LoxP recombination are identified by blue staining. Analysis of 5 individual mice reveals AdCre infection within a range of ovarian surface epithelium cells, bursa cells and granulosa cells. The right ovaries, not exposed to AdCre were used as negative controls and reveal no  $\beta$ -galactosidase positive cells.

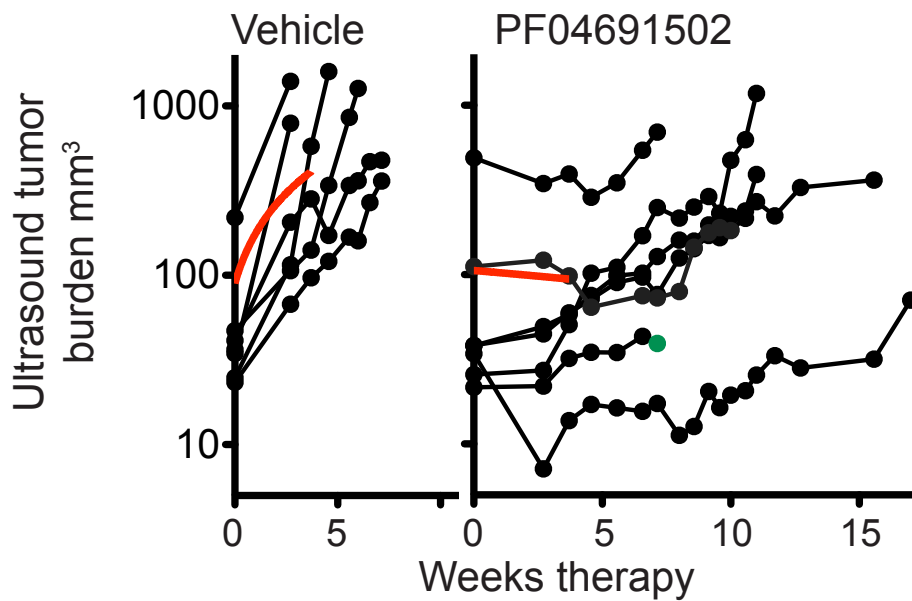


**Supplementary figure 6. *Pik3ca*<sup>H1047R</sup> in the ovarian surface epithelium leads to hyperproliferative changes.** (i) Non-AdCre exposed ovary from *Pik3ca*<sup>H1047R</sup> mutant mouse 12 months post AdCre, mag x4 (i). AdCre exposed ovary from *Pik3ca*<sup>H1047R</sup> mutant mice 12 months post AdCre from mouse 1 (ii and iii), mouse 2 (iv and v) and mouse 3 (vi and vii) at mag x4 (ii, iv and vi) and x20 (iii, v and vii).





**Supplementary figure 7: cDNA sequence of ovarian tumors.** (a) Expression of the *Pik3ca*<sup>H1047R</sup> mutant exon 20 in AdCre-induced ovarian tumors was confirmed by sequencing of cDNA. RNA was extracted from tumors arising in the AdCre-treated ovaries of mice heterozygous for *Pik3ca*<sup>H1047R</sup> allele and homozygous for *Pten*<sup>del/del</sup> by methods described in Sup Fig 4a.



**Supplementary figure 8. Measurement of *Pik3ca*<sup>H1047R</sup>; *Pten*<sup>del/del</sup> ovarian tumor volume by small animal ultrasound imaging following PF04691502 therapy.**

*Pik3ca*<sup>H1047R</sup>; *Pten*<sup>del/del</sup> mice were exposed to AdCre in the left ovarian bursa and therapy was begun at 10 weeks post AdCre, when ovarian tumor growth was evident by ultrasound (>20mm<sup>3</sup>). Serial ultrasound imaging was used to monitor changes in tumor volume of individual mice over time for each cohort. Blank lines indicate ultrasound tumor burden for each animal and the red line indicates the mean trend (linear regression curve) over the first 26 days of therapy. PF04691502 inhibited tumor growth, and delayed the onset of exponential growth observed with this model. Mice generally tolerated the drug well, however, 1 mouse on therapy (46 days) was sacrificed due to rapid weight loss unrelated to tumor burden (green circle).

## **Supplementary methods**

### **AdCre recombination in the ovary**

AdCre was prepared by methods previously described (1). Ovulation was synchronized by i.p. injection of 5U of pregnant mare serum gonadotropin (Intervet, Australia), followed by 5U human chorionic gonadotropin (Intervet) 48 hours later. 1.5d later, mice were anaesthetized using ketamine and xylazine (86 and 17 mg/kg, respectively) and a dorsal excision was made to expose the ovary. A 32-gauge needle was used to inject  $2.0 \times 10^8$  optical particle units of AdCre in 5 $\mu$ L (precipitate prepared in 1:1 DMEM and PBS/virus mix; supplemented with 0.2M CaCl<sub>2</sub>) into the ovarian bursa. The ovary was returned to the body and the incision sealed with sutures and staples.

### **Protein analysis**

Antibodies used in IHC were pAKT (S473, CS3787), pAKT (T308, CS4056), pRPS6 (S235/236, CS2211), PTEN (CS9559) from Cell Signaling Technology, Inhibin alpha (MCA951S, AbD Serotec), Cytokeratin AE1/AE3 and smooth muscle actin (1A4, DakoCytomation).

RIPA buffer used for Western blotting was 1mM EDTA; 1% NP40; 0.5% sodium deoxychlorate; 0.1% SDS; 50mM sodium fluoride; 1mM sodium pyrophosphate in PBS, supplemented with phosphatase inhibitor cocktail (Roche). Antibodies used for western blotting were pPDK1 (CS3061), pAKT (Ser473, CS9271), pAKT (T308; CS4056), AKT (CS9272), pRPS6 (CS2215), S6 (CS2217), pGSK3b (CS9336), GSK3b (CS9315),

pPRAS40 (CS2997), PRAS40 (CS2610), p4EBP1 (CS2855) and 4EBP1 (CS9977) each from Cell Signaling Technology and pan-actin (clone C4, MAB1501, Millipore).

### **$\beta$ -Galactosidase staining**

Tissues were fixed (2% paraformaldehyde/0.2% glutaraldehyde solution, followed by 20% sucrose solution) and frozen in OCT mounting medium and stored at -80°C. 10 $\mu$ m sections were cut onto superfrost+ slides and infected cells were identified by  $\beta$ -galactosidase staining (2) and counterstained with nuclear fast red. AdCre infected cells with successful LoxP recombination are identified by blue staining.

### **Genetic analysis of PI3K pathway in ovarian cancer**

Genetic analysis of *PIK3CA*, *PIK3R1*, *PTEN* and *KRAS* was performed on 87 primary epithelial ovarian tumours with both copy number and gene sequence information. Tissue samples were obtained through the Peter MacCallum Cancer Centre Tissue Bank or from patients presenting to hospitals in the south of England. This tumour cohort comprised a mixture of serous (n=45), endometrioid (grade 1 and 2 n=16, grade 3 n=13), mucinous (n=7) and clear cell (n=6) subtypes.

Tumour DNA was extracted from microdissected tissue and copy number values were generated from Affymetrix SNP 6.0 Mapping Arrays as described in Gorringer *et al* (3). Samples were assessed for any copy number change intersection with the genes *PIK3CA* and *PTEN*. Somatic mutations were identified by next generation sequencing as part of a larger study to be reported in full elsewhere. Briefly, 200 ng of tumour or matched blood

normal DNA was fragmented to ~200 bp (Covaris, Woburn, MA) and end repair and A-tailing performed according to the Illumina genomic DNA library preparation protocol (Illumina, San Diego, CA). Following this, DNA was ligated with one of 7 custom indexed adapters compatible with Illumina single end sequencing. Indexed DNA samples were pooled equally prior to PCR enrichment. All reagents used during library preparation were obtained from New England Biolabs (NEB, Ipswich, MA). A boutique exon capture (SureSelect, Agilent Technologies, Santa Clara, CA) was used to specifically enrich for all coding exons of *PIK3CA*, *PIK3RI*, *PTEN* and *KRAS* from genomic DNA libraries prior to next generation sequencing. Capture probes were designed by submitting genomic coordinates to eArray (Agilent) and used default parameters. Solution hybridization, washing, elution and amplification were performed according to the manufacturer's instructions. Each target-enriched DNA library was sequenced on two lanes of an Illumina GAIIx, generating 75 bp single end sequence reads. Image analysis and base calling was performed using the Genome Analyser Pipeline v1.6. Sequencing reads were aligned to the human reference genome (GRCh37/hg19) using BWA (4) and any unmapped reads were aligned with Novoalign (Hercus, 2009). Reads were then locally realigned with GATK (5), point mutations and indels called with GATK and Dindel (6) respectively and variants were annotated with Ensembl v56. Matched normal samples were used to distinguish germline variation from somatic alterations in tumour samples. All somatic non-silent variants were confirmed by PCR amplification and capillary electrophoresis on the ABI3130 Genetic Analyser using BigDye Terminator v3.1 sequencing chemistry (Applied Biosystems, Foster City, CA).

## Supplementary References

1. Kanegae Y, Lee G, Sato Y, et al. Efficient gene activation in mammalian cells by using recombinant adenovirus expressing site-specific Cre recombinase. *Nucleic Acids Res.* Oct 11 1995;23(19):3816-3821.
2. Pearson HB, McCarthy A, Collins CM, Ashworth A, Clarke AR. Lkb1 deficiency causes prostate neoplasia in the mouse. *Cancer Res.* Apr 1 2008;68(7):2223-2232.
3. Gorringer KL, Ramakrishna M, Williams LH, et al. Are there any more ovarian tumor suppressor genes? A new perspective using ultra high-resolution copy number and loss of heterozygosity analysis. *Genes Chromosomes Cancer.* Oct 2009;48(10):931-942.
4. Li H, Durbin R. Fast and accurate short read alignment with Burrows-Wheeler transform. *Bioinformatics.* Jul 15 2009;25(14):1754-1760.
5. McKenna A, Hanna M, Banks E, et al. The Genome Analysis Toolkit: a MapReduce framework for analyzing next-generation DNA sequencing data. *Genome Res.* Sep 2010;20(9):1297-1303.
6. Albers CA, Lunter G, Macarthur DG, McVean G, Ouwehand WH, Durbin R. Dindel: Accurate indel calls from short-read data. *Genome Res.* Oct 27 2010.

Hercus C (2009). <http://www.novocraft.com>